Hybridization-mediated anisotropic coupling in plutonium compounds

Amitava Banerjea, Bernard R. Cooper, and Pradeep Thayamballi
Department of Physics, West Virginia University, Morgantown, West Virginia 26506-6023
(Received 19 March 1984)

The magnetic behavior of a class of cerium and light actinide compounds containing moderately delocalized f electrons has been explained on the basis of an anisotropic two-ion interaction that arises from the hybridization of band electrons and the f electrons. This theory, first developed by Siemann and Cooper for cerium compounds using the treatment of Coqblin and Schrieffer for the hybridization, was later generalized by Thayamballi and Cooper to f^n systems in the L-S and j-j coupling limits. We here extend the theory to the case of intermediate intraionic coupling and further include the possibility of long-period antiferromagnetic structures. In particular, we have considered the $Pu^{3+}(f^5)$ ion in PuSb. The theory reproduces the experimentally observed magnetic behavior of PuSb quite closely, predicting a phase transition from a low-temperature ferromagnetic phase to a long-period antiferromagnetic phase at about 75 K, for a fitting to a Néel temperature of 85 K, with ordered moments close to the experimental values. However, while the modulation in the long-period antiferromagnetic phase has been experimentally observed to be longitudinal, the theory predicts a transverse modulation with moments aligned along the cube edge. We also present the $T=0$ magnetic excitation spectrum in the ferromagnetic phase calculated on the basis of this theory using the random-phase approximation.

I. INTRODUCTION

The heavier monopnictides (antimonides and bismuthides) of cerium and the light actinides (U, Np, and Pu) which crystallize in a NaCl structure show a number of unusual magnetic structures with extremely large anisotropy along the cube edge.[1-4] In CeSb there are many different antiferromagnetic structures below the Néel temperature (16 K) with ferromagnetic {001} planes as the basic units.[5] PuSb undergoes an initial ordering to a long-period antiferromagnetic phase at the Néel temperature of 85 K and undergoes a first-order transition[4] to a ferromagnetic phase at 75 K.

The static and dynamic magnetic properties of cerium compounds have been successfully explained[6-9] as arising from a highly anisotropic interionic interaction arising from the resonant hybridization of moderately delocalized f electrons with band electrons. This hybridization in $Ce^{3+}(f^1)$ compounds, which was first treated by Coqblin and Schrieffer[10] to explain the behavior of dilute cerium alloys, has been extended by Thayamballi and Cooper[11-13] to the general case of f^n ions and applied to $U^{4+,3+}(f^2,f^3)$ compounds and, more recently, to the case of $Pu^{3+}(f^5)$ compounds such as PuSb.

In this theory of hybridization-mediated anisotropic two-ion interaction the angular dependence of the interaction depends on the f occupation number and on the nature of the intraionic coupling. Thayamballi and Cooper have reported the results of calculations for the f^5 system in two limiting cases of intraionic coupling, j-j coupling and L-S coupling.[12,13] While the magnitude of the moment and the behavior of the magnetization with temperature were well reproduced in the L-S limit, no phase transition from a ferromagnetic phase to an antiferromagnetic one could be obtained. On the other hand, in the limit of j-j coupling, a transition to antiferromagnetic behavior was obtained, but the size of the moment and the variation of the magnetization with temperature in the ferromagnetic phase could not be reproduced.

In this paper we will describe extensions of previous work[12,13] on the behavior of the PuSb to the case of intermediate coupling (IC) within the $Pu^{3+}(f^5)$ ion. Other than the fact that more terms are involved, the calculations for the case of intermediate coupling are similar in principle to those in the L-S coupling case. In Sec. II and in Appendix A we briefly review the treatment of intermediate intraionic coupling following Judd.[14] Section III contains a brief review of the model of hybridization-mediated interionic coupling in the f^n system (which has been presented in detail elsewhere[12]). We have also investigated the magnetic excitation behavior in the intermediate-coupling case; this will be discussed in Sec. IV. Results and discussion are presented in Sec. V.

In the present intermediate-coupling (IC) calculations we have included the possibility of long-period planar antiferromagnetic structures which were not considered earlier. We have also investigated the effect of including such longer-period antiferromagnetic structures in the limit of L-S coupling. The inclusion of such structures has been motivated by two factors. First, since the ground state is ferromagnetic in the situation pertinent to PuSb, antiferromagnetic structures built out of periods having several successive ferromagnetically aligned planes (with compensating sequences of planes with antiparallel moments) should move closer to the ground state in energy as the number of planes in each ferromagnetic sequence is increased, and this should increase the likelihood of a thermal transition to an antiferromagnetic state.

The second motivating factor is the experimental observation that PuSb undergoes a transition to an antiferromagnetic phase that is characterized by a long-wavelength modulation.[2]

In agreement with spectroscopic evidence and earlier calculations,[15] we find that the IC ground state of the Pu^{3+} ion is composed primarily of the ^6H state (which is the ground state in the L-S coupling limit) and four ^4G states. Hence, it is not surprising that the results of the L-S limit should be close to experimental results and that the results for the case of intermediate coupling should be close to those obtained in the L-S coupling limit. The change to intermediate coupling does not lead to any significant qualitative differences in the results. We have found that the inclusion of a long-period $(+ + + - - -)$ antiferromagnetic structure in the calculations makes it possible to reproduce the experimental magnetization-versus-temperature (M-T) curves quite closely and at the same time obtain a first-order phase transition to the long-period antiferromagnetic structure at the correct temperature. There is a significant disagreement with experiment, however, in that the long-period antiferromagnetic structure is experimentally found to be characterized by a longitudinal modulation of the magnetization[2] (modulation wave vector parallel to the moment direction), whereas the theoretical calculations indicate a transverse modulation (moments along the cube edge, but perpendicular to the modulation wave vector). This discrepancy and its implications are discussed in Sec. V.

II. INTERMEDIATE COUPLING

The problem of determining the eigenstates and eigenenergies of many-electron atoms, particularly those in which there are two or more electrons outside a closed configuration, is an old one particularly familiar to spectroscopists.[16] The Coulomb interaction between the electrons, given by

$$\mathscr{H}_c = \sum_{\substack{i,j \\ i>j}} \frac{e^2}{r_{ij}} , \tag{1}$$

and the coupling of the orbital angular momentum to the spin angular momentum (spin-orbit coupling), given by

$$\mathscr{H}_{\text{s.o.}} = \sum_i \xi(r_i)\vec{\mathrm{s}}_i \cdot \vec{\mathrm{l}}_i , \tag{2}$$

have to be considered in addition to an effective central potential. These interactions are generally treated as perturbations on the central potential. The problem is relatively easy to solve at the two limiting cases where either the Coulomb interaction or the spin-orbit coupling dominates. These limiting cases are the familiar Russel-Saunders or L-S coupling limit where the Coulomb interaction dominates and the spin-orbit interaction is neglected, and the j-j coupling limit where the spin-orbit coupling dominates and the Coulomb interaction is neglected. Although most atoms can be described reasonably well by one or the other limiting case (atoms lighter than the actinides by the L-S and the heaviest actinides by the j-j), the correct description of any atom is to be found in an IC scheme where both the Coulomb repulsion and the spin-orbit coupling are simultaneously taken into account. Such intermediate coupling effects are known to be significant for the lighter actinides.

In order to obtain the eigenstates and energies in the IC scheme it is convenient to start with a familiar set of basis vectors. The problem then becomes one of finding the matrix elements of the Coulomb interaction and the spin-orbit coupling in this basis, and of then diagonalizing the resultant matrix. Since most atoms lie near the L-S coupling limit it is common to use the eigenstates of the L-S coupling limit as the initial basis set for the problem of intermediate coupling. In the limit of L-S coupling, the total angular momentum of the atom L, the total spin S, and the total angular momentum J are all good quantum numbers. In the intermediate-coupling case, only J is a good quantum number. Hence, as one proceeds to intermediate coupling from the L-S limit by turning on the spin-orbit coupling, J remains a good quantum number, and if the spin-orbit coupling is small (as it is in Pu^{3+}), it is reasonable to assume that the lower-energy levels do not cross, and the value of J for the IC ground state is the same as that of the L-S ground state. It is also known from experiments that the ground state of the Pu^{3+} ion has the same J $(=\frac{5}{2})$ as the Hund's-rule-favored (L-S coupled) ground state. This fact can be utilized to reduce the calculations significantly.

While the calculation of the matrix elements of the spin-orbit coupling is straightforward in most cases involving nonequivalent electrons outside a closed shell, for equivalent electrons outside a filled shell (as in our f^n case) the possibility of more than one state being described by the same values of L and S raises the problem of defining a state. Consequently, attention has been focused on the problem of defining other quantum numbers which will serve to distinguish states with the same values of L and S. This problem has been addressed by Racah[17] using the theory of continuous groups. An account of Racah's methods has been given by Judd.[14] The motivation for the method comes from the fact that under three-dimensional rotations the $2L+1$ components of a term with given S and M_S transform according to the representation D_L of the group R(3). Then the objective is to find a group G of operations which includes the operations of R(3) as a subgroup so that the irreducible representations of G can be used as additional labels for the states. If the terms can then be divided into sets such that the eigenfunctions of each set form the basis for an irreducible representation of G, and different terms with the same L and S values belong to different irreducible representations, then one has appropriate labels to distinguish all the states. In the case of f electrons a hierarchy of two such groups, R(7) and G(2), are sufficient to provide appropriate distinguishing labels. A part of the succession of groups and subgroups may be represented as

$$\mathrm{R}(3) \subset \mathrm{G}(2) \subset \mathrm{R}(7) \subset \mathrm{SU}(7) . \tag{3}$$

An ordered trio of integers $W \equiv (w_1, w_2, w_3)$ is used to label the irreducible representations of G(2), while an ordered pair of integers $U \equiv (u_1, u_2)$ labels the irreducible

representations of R(7). Occasionally, two different states may occur that have the same values of $WUSL$ and we will use a label τ to distinguish these. Any state can then be distinctly labeled as $|WU\tau LSM_L M_S\rangle$. The matrix elements of the spin-orbit Hamiltonian of Eq. (2) can be obtained using the properties of these irreducible representations. The details of these calculations are presented in Appendix A.

The matrix elements of the Coulomb interaction for f^n configurations have been worked out by a number of authors. These matrix elements are evaluated in terms of four radial integrals which are usually treated as experimentally determined parameters. We have used the matrix elements determined by Wybourne[18] and the values of the radial integrals quoted by Chan and Lam.[15]

Upon diagonalizing the sum of the Coulomb and spin-orbit matrices, the ground state is found to be composed primarily of the ^6H term ($\sim 72\%$), which is the L-S ground state, and four ^4G terms ($\sim 23\%$). These numbers differ somewhat from those found by Chan and Lam (67% and 25%). One possible source of this discrepancy is that we have not been able to locate all the requisite tables of the factors of the coefficients of fractional parentage. This leads to a spin-orbit matrix that is only approximately correct, and this might explain the discrepancy between our results and those of Chan and Lam. Since, as described below, we retain only the ^6H and ^4G terms, and vary their percentages slightly to see if this affects our results, there was no reason to pursue this slight discrepancy.

A ground-state wave function $|\mathcal{G}M_J\rangle$ with a given value of M_J may be approximately written as

$$|\mathcal{G}M_J\rangle = C_H\,|^6H_{5/2}M_J\rangle + C_G\left[\sum_{\alpha=1}^{4} y_\alpha\,|\alpha\,^4G_{5/2}M_J\rangle\right] + \cdots , \tag{4}$$

where $\alpha \equiv WU$ distinguishes the four ^4G states. Here, and in subsequent calculations, we neglect the contributions from all the other terms and scale up the total proportions of the ^6H and ^4G terms ($|C_H|^2$ and $|C_G|^2$) to complete 100%. The relative phases of all terms and the relative contributions of the four ^4G states are left unchanged.

The wave function of a many-electron state can be expressed as a totally antisymmetrized determinantal product of one-electron wave functions commonly known as a Slater determinant (SD). The elegant group-theoretical techniques that we have just referred to were developed by Racah and others in order to avoid having to deal with such SD's as much as possible and thus keep calculations from becoming too cumbersome and complicated. However, in the case of f^n systems, to determine the scattering coefficients $A_{mm'}^{MM'}$, which arise in our theory[11,12] from one-electron transfers, we need to have the ground state expressed as a linear combination of SD's. The details of how the relevant linear combinations are obtained can be found in Appendix B.

III. HYBRIDIZATION-MEDIATED INTERACTION

The methodology of treating f-electron—band-electron hybridization in terms of resonant scattering was first developed by Coqblin and Schrieffer[10] for cerium impurity ions, and later extended by Siemann and Cooper[6,7] and Yang and Cooper[8,19] to develop the hybridization-mediated anisotropic two-ion interaction in cerium compounds, and by Thayamballi and Cooper[11–13] to treat the two-ion interaction in compounds of the light actinides. Here we will briefly review the theory. The basis for the theory is provided by the Anderson model[20] with its mixing Hamiltonian,

$$\mathcal{H}_{\rm mix} = \sum_{k,m} (V_k b_{km}^\dagger c_m + V_k^* c_m^\dagger b_{km}) . \tag{5}$$

Here V_k is the strength of the mixing potential, and $b^\dagger$ (b) and $c^\dagger$ (c) denote creation (destruction) operators for the band and ionic states, respectively. The mixing potential is assumed to be spherical, and resonant mixing occurs between the localized f electrons and the f partial-wave component of the bands. Upon applying the Schrieffer-Wolff[21,22] transformation the scattering contribution transforms to an effective electron scattering Hamiltonian. When this scattering Hamiltonian is treated in second-order perturbation theory, one obtains an interionic interaction which is similar, in essence, to the Ruderman-Kittel[23] interaction, information being transmitted between ions by the scattered band electrons. In the f^1 case Siemann and Cooper[7] have shown that the predominant two-ion coupling comes from the $m_l=0$ (quantization along the interionic axis) part of the localized f wave function, corresponding to the piling up of charge along the interionic axis. This is true as long as the mixing is spherical.

For treating the single-site band-f hybridization in the f^n case, Thayamballi and Cooper[12] have adopted the single-electron exchange scattering methodology developed by Coqblin and Schrieffer[10] for the f^1 case. Then, in the f^n case, as in the f^1 case, the predominant contribution to the two-ion interaction comes from scattering events in which the exchanged electron has $m_l=0$. For that reason, only such scattering events are considered in finding the two-ion interaction, and one uses a single-site scattering Hamiltonian given by

$$\mathcal{H}_{ns} = -\sum_{k,k'} g_{kk'} \sum_{M,M'} \sum_{\substack{m,m' \\ =\pm 1/2}} A_{mm'}^{MM'} d_{M'}^\dagger d_M b_{k'm'}^\dagger b_{km} , \tag{6}$$

where $A_{mm'}^{MM'}$ is the scattering coefficient for the event, $M(m)$ and $M'(m')$ are the initial and final magnetic quantum numbers of the ion (band electron), $d^\dagger$ (d) is the creation (destruction) operator for the appropriate ionic state, and $g_{kk'}$ is the coupling coefficient which depends on the mixing strength $|V|^2$ and the energies of the initial, final, and intermediate states. New scattering coefficients can be defined which retain only the exchange and relative direct scattering contributions,

$$\mathscr{A}^{MM'}_{mm'} = A^{MM'}_{mm'} - \frac{\delta_{MM'}\delta_{mm'}}{2J+1}\sum_{N} A^{NN}_{mm} \ . \tag{7}$$

Then, treating the single-site scattering Hamiltonian to second order one obtains the interaction between ions at sites i and j as

$$\mathscr{H}_{ij} = -E_{ij}\sum_{\substack{M,M'\\N,N'}} J^{MM'}_{NN'} L^{(i)}_{M'M} L^{(j)}_{N'N} \ , \tag{8}$$

where

$$J^{MM'}_{NN'} = \sum_{\substack{m,m'\\=\pm 1/2}} \mathscr{A}^{MM'}_{mm'} \mathscr{A}^{NN'}_{m'm} \tag{9}$$

and

$$L_{\alpha\beta} = |\alpha\rangle\langle\beta| \ . \tag{10}$$

The indices m and m' are summed over $\pm\frac{1}{2}$, and M, M', N, N' are summed over all possible M_J values for the ground-state multiplet of the ion. E_{ij} is a range function which, for free-electron bands, is identical with the Ruderman-Kittel range function.

At present we have treated the interaction range factors E_{ij} as phenomenological parameters with E_n giving the strength of the interaction with the nth near neighbors. Since a small isotropic (Heisenberg) Ruderman-Kittel—type interaction, defined through

$$\mathscr{H}^{\text{Heis}}_{ij} = -\frac{H_{ij}}{|\vec{\mathbf{J}}|^2}(\vec{\mathbf{J}}_i\cdot\vec{\mathbf{J}}_j) \ , \tag{11}$$

is also expected to be present, we have also included parameters, H_n giving the Heisenberg interaction with the nth near neighbor. At this point in the development the ionic states are labeled by their magnetic quantum numbers with quantization along the interionic axis. In order to treat magnetic ordering in a lattice of ions, all such states must be transformed to a common quantization axis through the appropriate transformation.[6,24] This two-ion interaction is treated in a molecular-field formalism in order to obtain equilibrium behavior and to study phase transitions.

IV. EXCITATIONS

The two-ion interactions of the system can be written[19] as

$$\mathscr{H} = -\sum_{\vec{q}}\sum_{\substack{\mu,\nu,\\ \epsilon,\sigma}} J^{\epsilon\sigma}_{\mu\nu}(\vec{q}) L^{\vec{q}}_{\mu\nu} L^{-\vec{q}}_{\epsilon\sigma} \ , \tag{12}$$

where μ, ν, ϵ, and σ refer to the M_J states referred to the crystalline coordinate system; the $J^{\epsilon\sigma}_{\mu\nu}(\vec{q})$ depend on the two-ion interaction constants, the $J^{MM'}_{NN'}$ defined in Eq. (8), and the rotational transformations between each interionic axis and the crystalline coordinate system; the $L^{\vec{q}}_{\mu\nu}$ are Fourier transforms of the transition operators defined in Eq. (10). The equilibrium magnetic state is obtained by treating the Hamiltonian $\mathscr{H}$ in Eq. (12) in the mean-field (MF) approximation. The transitions between the MF states are induced by the difference between the Hamiltonian of Eq. (12) and the mean-field Hamiltonian $\mathscr{H}_{\text{MF}}$,

$$\mathscr{H}_{\text{MF}} = \sum_i \sum_m \mathscr{E}^i_m L^i_{mm} \ , \tag{13}$$

where we have denoted the MF states by lower-case Latin letters, and $\mathscr{E}^i_m$ denotes the energy of the MF state $|m\rangle$ on site i.

To study the excitations of the system we project the Hamiltonian $\mathscr{H}$ into the MF manifold.[9,19] At $T=0$ we need only consider the set of operators that take the system from, or to, the MF ground state (L_{1m} or L_{m1}, $m\neq 1$). The dynamics of the system is found by using the equation-of-motion technique. For the ferromagnet, the commutators with the MF Hamiltonian are

$$[\mathscr{H}_{\text{MF}}, L^{\vec{q}}_{mn}] = (\mathscr{E}_m - \mathscr{E}_n)L^{\vec{q}}_{mn} \ . \tag{14}$$

In calculating the commutator with $\mathscr{H}'$ ($=\mathscr{H}-\mathscr{H}_{\text{MF}}$), we use the random-phase approximation (RPA) to decouple terms with more than one L_{mn} operator. This yields

$$[\mathscr{H}', L^{\vec{q}}_{mn}] = 2(\langle L^0_{mn}\rangle - \langle L^0_{nn}\rangle)\sum_{s,t} J^{st}_{nm}(\vec{q}) L^{\vec{q}}_{st} \ . \tag{15}$$

The thermal average $\langle L^0_{mm}\rangle$ is unity if m is the ground state ($m=1$) and zero otherwise. Upon diagonalizing the resulting 10×10 dynamical matrix (upward and downward transitions between the ground state and each of the five excited states), we obtain five modes at energy gain and five at energy loss.

V. RESULTS AND DISCUSSION

Since the ground state of the L-S coupling limit is the predominant component of the IC ground state (which we take as 75% ^6H and 25% ^4G), it is not surprising that the results in the two cases should be very similar. In fact, the scattering coefficients $\mathscr{A}^{MM'}_{mm'}$ for the IC case are not very much different from those of the L-S case. Figure 1 shows the free energies at $T=0$ of the low-lying states for the L-S case, the IC case and a case where the proportion of the ^4G states has been increased to 35%. All three cases in Fig. 1 are for $E_1=E_2=|E_1|$. In all antiferromagnetic structures the modulation is taken to be along the [001] direction. The 3,3 structure is one which has ferromagnetic planes in a three-up—three-down ($+++---$) arrangement. The moments on the three planes in one sequence of three "up" planes or three "down" planes are not identical, but are symmetrically arranged, i.e., the two outer planes have the same moments, which differ from the moment on the central plane in any sequence of three ferromagnetically aligned planes. The ratio of the moment on one of the outer planes to that on the central plane is close to unity at zero temperature, but changes significantly as the temperature is raised.

At zero temperature the ground state for both the IC case and the L-S case is a ferromagnetic structure with nearly saturated moments aligned along the cube edge. As expected, the 3,3 structure is closer in energy to the ferromagnetic state than the type-I or -IA structures, and a transition to such a structure is more likely than a transition to a type-I or -IA structure. It is interesting to note that of the three type-I structures considered here (with different directions of moment alignment), the one with the moment along the face diagonal has the lowest energy, so that it is not possible to produce a transition to a type-I structure with the experimentally observed anisotropy favoring cube-edge moment alignment. Of the three type-IA structures and of the three 3,3 structures, the ones

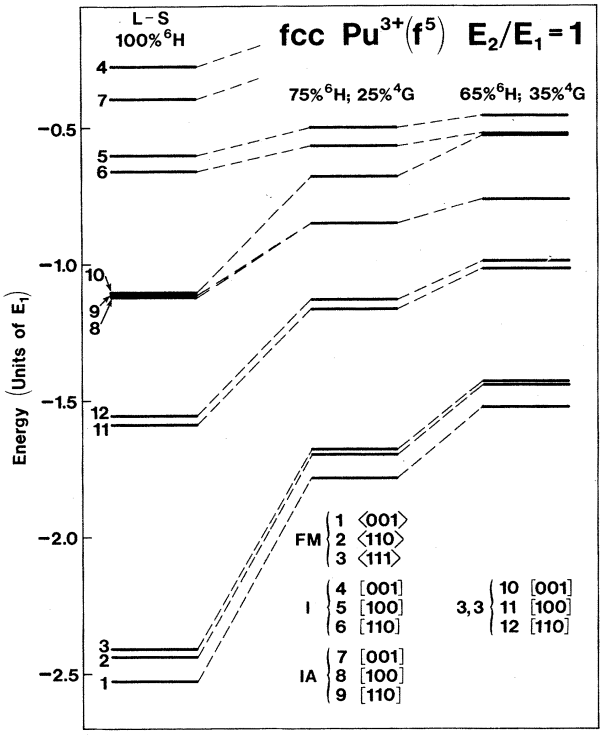

FIG. 1. Free energies at zero temperature of different magnetic structures for the cases of L-S coupling, intermediate coupling (75% ^6H and 25% ^4G), and a state with 65% ^6H and 35% ^4G with $E_1=E_2$. FM denotes ferromagnetic structures, I and IA denote antiferromagnetic structures of types I and IA, respectively, and 3,3 denotes a three-up—three-down antiferromagnetic structure.

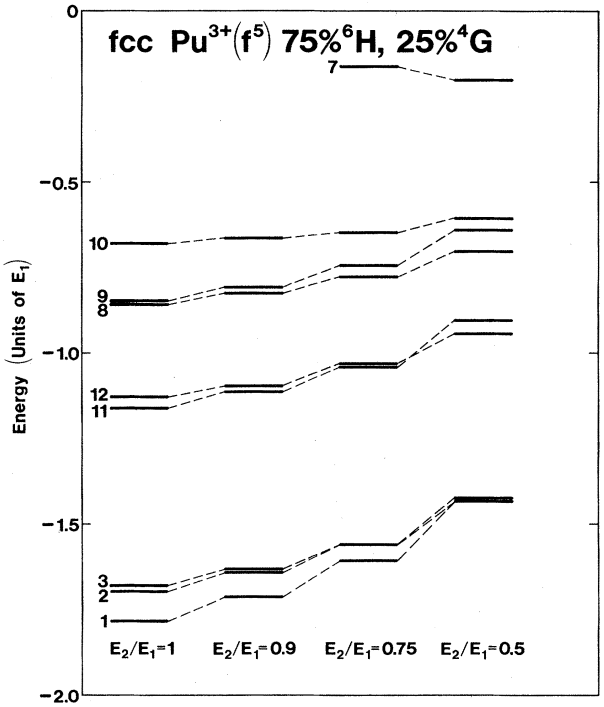

FIG. 2. Zero-temperature free energies of different magnetic structures for different values of E_2/E_1 in the intermediate-coupling case. The structures are labeled as in Fig. 1. For $E_2/E_1=0.5$, structure 2 has the lowest energy.

with lowest energy are the ones with moments along a cube edge perpendicular to the direction of modulation. This characteristic foreshadows our finding that the antiferromagnetic structure to which the ferromagnetic one undergoes a transition is characterized by transverse, rather than longitudinal, polarization.

The effect of changing the ratio E_2/E_1 is shown in Fig. 2, and Fig. 3 shows the effect of including crystal-field splitting. Changing the ratio E_2/E_1 or introducing a crystal-field splitting does not make the longitudinally polarized phase (state 10) lower in energy than the transversely polarized one (state 11). Indeed, as we can see from Fig. 2, upon decreasing E_2/E_1 the ground state goes from a cube-edge ferromagnet (state 1) to a face-diagonal ferromagnet (state 2). (In Fig. 2, state 2 is actually slightly lower than states 1 and 3, with which it appears to coincide.) Upon increasing the ratio E_2/E_1 the longitudinally polarized antiferromagnetic phase moves even further above the transversely polarized one. Upon including a relatively small positive crystal field, the ground state changes from a cube-edge ferromagnet to a body-diagonal ferromagnet. For a negative crystal field, as the crystal field becomes increasingly negative the most important effect is that the magnitude of the moment in the ferromagnetic structure decreases slightly. We have utilized this feature in matching the experimentally observed[25] f moment in PuSb.

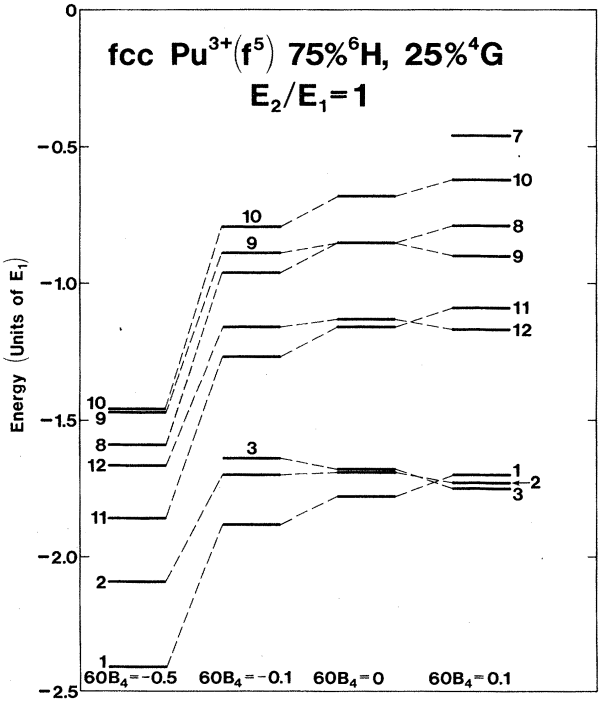

FIG. 3. Zero-temperature free energies for different magnetic structures with $E_2/E_1=1$ and varying values of the crystal-field parameter (Ref. 26) B_4. The structures are labeled as in Fig. 1.

The addition of a small antiferromagnetic H_3 ($-0.028E_1$ for IC), a moderate antiferromagnetic E_3 ($-0.32E_1$ for IC and $-0.33E_1$ for L-S coupling), or a somewhat larger E_4 ($-0.54E_1$ for IC with E_3 set equal to zero) produces a transition to a 3,3 structure (with a moment along the cube edge, but perpendicular to the modulation direction) at about 75 K for a Néel temperature of 85 K (i.e., choosing E_1 to fit $T_N=85$ K). If a crystal field is also included, the value of the antiferromagnetic coupling required changes slightly. It should also be noted that upon introducing an antiferromagnetic anisotropic (E_n) or isotropic (H_n) interaction with the third or further near neighbors in either the IC or the L-S coupling case, the [110] type-IA structure is favored over the [100] and [001] structures. Consequently, it is not possible[12] to reproduce a transition to a type-I or -IA antiferromagnetic structure with the correct moment anisotropy by including a negative E_3 or H_3.

The variation of the moment with temperature for intermediate coupling (75% ^6H and 25% ^4G) with $E_1=E_2=|E_1|$ and $E_3=-0.32E_1$ is shown in Fig. 4 along with the experimental magnetization results of Spirlet, Rebizant, Vogt, and Mueller.[4,13] For the antiferromagnetic phase we have plotted the average of the moments of the three ferromagnetically aligned planes. (There are no available experimental moment values in the antiferromagnetic phase as yet.) The variation of moment with temperature in the other cases (IC with H_3 or E_4 or L-S coupling with E_3 or E_4 or H_3) is almost identical in the ferromagnetic phase (apart from an overall scaling of the moment in the L-S case which arises because the g factor for the L-S coupling case is smaller than that in the IC case), and shows only minor differences in the antiferromagnetic phase.

The g factor for the intermediate-coupled state is given in terms of the g factors of the component L-S states as[16]

$$g(J)=\sum_{\tau,S,L} g(SLJ)\,|\,(\tau SLJ\,|\,J)\,|^2 . \tag{16}$$

For the IC ground state (75% ^6H and 25% ^4G) of Pu^{3+} this equation yields a value of $g=\frac{5}{14}$, which is 25% higher than that for the L-S—coupled ground state. Thus, the theoretically predicted moment for the IC state at zero temperature (with no crystal field) is $0.89\mu_B$, whereas the $T=0$ moment in the L-S—coupled case is about $0.71\mu_B$. The f moment as determined from neutron-scattering experiments[25] is $(0.76\pm0.03)\mu_B$, while the overall moment (presumably including antiparallel band-polarization effects) has been determined from magnetization experiments[4,13] to be $0.67\mu_B$. In the j-j coupling limit the $T=0$ moment would be much larger (about $2.1\mu_B$) than the experimental moment. We have been able to reproduce the experimentally determined low-temperature moment[25] of $0.76\mu_B$ as well as a first-order transition from a ferromagnetic to an antiferromagnetic phase at the correct temperature with $E_1=E_2=|E_1|=129.8$ K, $B_4=-(1.3/60)E_1$, and $H_3=-0.0278E_1$. The value of the crystal-field parameter[26] B_4 has been chosen (relative to E_1) so as to match the low-temperature f moment determined from neutron experiments. Figure 5 shows the variation of the theoretical and experimental (magnetization) moments with temperature. Again, for the antiferromagnetic phase the averaged sublattice moment (which cannot be measured in a mag-

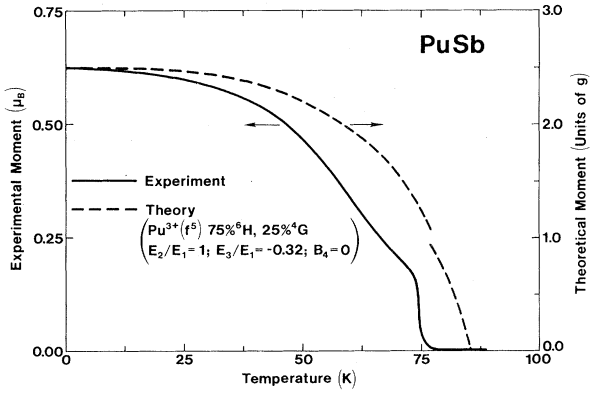

FIG. 4. Variation of magnetic moment with temperature. The experimental curve (solid line) is from the magnetization experiments (Refs. 4 and 13) and the theoretical curve (dashed line) shows the predicted f moment in the intermediate-coupling case with $E_1=E_2$ and $E_3=-0.32E_1$. (To match the experimental value of T_N, $E_1=90$ K.) The theoretically predicted average sublattice moment (see text) has been plotted for the antiferromagnetic phase. The theoretical moments must be multiplied by g ($=\frac{2}{7}$) to be compared with the experimental values.

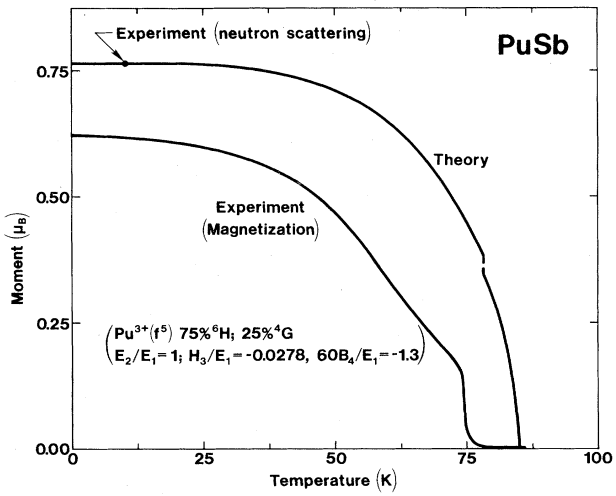

FIG. 5. Variation of magnetic moment with temperature. The experimental magnetization curve is the same as in Fig. 4 (Refs. 4 and 13). We also show the experimental f moment from recent neutron experiments of Lander *et al.* (Ref. 25). The theoretical curve shows the predicted f moment in the intermediate-coupling case with $E_1=E_2$, $H_3=-0.0278E_1$, and $B_4=-(1.3/60)E_1$. In order to match the experimental T_N, we have set $E_1=129.8$ K, which gives $B_4=-2.81$, and hence $\Delta_{CF}=-1012$ K; negative splitting means Γ_8 is lower than Γ_7. The value of B_4 has been chosen (relative to E_1) so as to match the f moment determined from neutron experiments. The theoretical moments include the g factor ($=\frac{5}{14}$). The average sublattice moment has been plotted for the antiferromagnetic phase.

netization experiment) has been plotted. The fact that the crystal-field parameter[26] B_4 is negative means that the Γ_8 state is lower in energy than the Γ_7 state. The value of E_1 (around 130 K) required to match the experimental Néel temperature implies a crystal-field splitting of about 1000 K.

A large magnetic field is required to destroy the cube-edge anisotropy in PuSb. (Experimentally, this field is known to be greater than 100 kOe.[4,13]) In the model system with $E_1=E_2=|E_1|$ and $E_3\sim-0.3E_1$, upon applying a magnetic field along the $\langle 111\rangle$ direction at zero temperature, the moment of the IC or L-S coupling $\langle 001\rangle$ ferromagnet gradually tilts toward the $\langle 111\rangle$ direction until, at about 1 MOe, there occurs a first-order phase transition to a ferromagnetic phase, with moments aligned along the $\langle 111\rangle$ direction. In the model case with $E_1=E_2$ and $H_3=-0.028E_1$, the magnitude of the field at which this transition occurs is $\gtrsim$ 600 kOe.

Figure 6 shows the predicted magnetic excitation spectrum, at $T=0$, for the IC case with $E_1=E_2=|E_1|$, $B_4=-(1.3/60)E_1$, and $H_3=-0.0278E_1$. Because the crystal-field splitting is large, the MF energy levels are grouped into a quartet and a doublet. The Γ_8 quartet and the Γ_7 doublet are further split by the hybridization-mediated interaction. The L_{31}, L_{41}, and L_{51} modes are transverse excitations. The most intense of these, L_{41}, has an excitation energy of about 250 K at the Γ point (choosing E_1 to match the experimental T_N for PuSb) and increases in energy as we approach the X points. The anisotropy of the excitations between the directions parallel and perpendicular to the moment direction is small (about 10% difference in energy at the X points).

A number of points are quite clearly made by the results presented above. First, it is clear that while going to intermediate intraionic coupling brings the antiferromagnetic structures closer in energy to the ferromagnetic one at zero temperature and increases the magnitude of the moment, the behavior of the IC system is not drastically different from that of the L-S system. On the other hand, the long-period antiferromagnetic structures play a crucial role in shaping the phase diagram of the system since they provide antiferromagnetic states of lower free energy. In considering the possibility of such long-period antiferromagnetic structures, it is necessary to have long-range (to third or fourth near neighbors) antiferromagnetic coupling in order to stabilize the long-period antiferromagnet over the correct temperature range.

As we have already noted, the predicted polarization of moment in the long-period antiferromagnetic structure is transverse to the modulation direction of the structure, whereas experiments have determined the polarization to be longitudinal. From Figs. 2 and 3 it is clear that changing the crystal-field parameter or the ratio E_2/E_1 does not bring the longitudinally polarized antiferromagnetic structure lower in energy than the transversely polarized one, though on reducing E_2/E_1 the gap between the two is reduced slightly. The transverse polarization is a fine detail characteristic of the $Pu^{3+}(f^5)$ system near the L-S limit when the Pu^{3+} ions are coupled via hybridization with the band electrons. On the other hand, in the limit

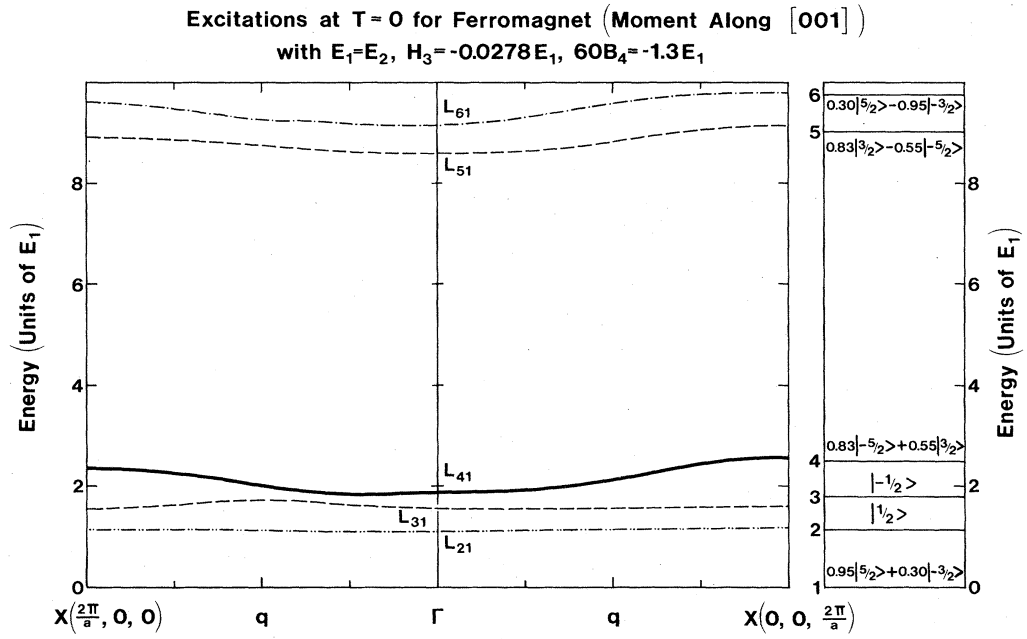

FIG. 6. Dispersion curves for excitations in the ferromagnetic phase at $T=0$ with intermediate coupling, $E_1=E_2=|E_1|$, $H_3=-0.0278E_1$, and $B_4=-(1.3/60)E_1$ for $\vec{q}$ along the [100] and [001] directions (parallel and perpendicular to the moment direction, respectively). $E_1=129.8$ K to match experimental T_N. The solid curve shows the most intense mode (that which is likely to be observed experimentally using the same criterion as in Ref. 9). The solid and dashed curves indicate excitations transverse to the moment direction. Other curves show the longitudinal (dashed-dotted) and quadrupolar (dashed—double-dotted) excitations. The energy levels of the molecular-field (MF) states and their compositions in terms of the angular momentum eigenstates (quantized along [001]) are shown on the far right. The modes L_{mn} are labeled by the corresponding dominant transitions between these MF levels.

of j-j intraionic coupling, as shown by Thayamballi and Cooper,[12,13] the behavior of the $Pu^{3+}(f^5)$ system would be the same as that of the $Ce^{3+}(f^1)$ system. Thus, the experimental polarization indicates that the behavior of the plutonium in the monopnictides is even more ceriumlike than our theory yields. Either we are not capturing the full subtlety of the intraionic coupling—our way of combining intraionic correlation and hybridization with the bands[12] may be a bit too crude—or there may be some other feature being omitted, such as the cubic part of the mixing potential, that will supply the necessary correction. In a sense, having the theory be more j-j—like might give the longitudinal polarization because this would give a more ceriumlike interionic interaction. It must be noted that we cannot reach the j-j coupling limit simply by increasing the proportion of ^4G states because as the ratio of the spin-orbit—coupling parameter to the electrostatic interaction parameters is increased, other states (such as ^2F and ^2D) which have been ignored here begin to contribute significantly to the ground state. Of course, as we move closer to the j-j limit, the magnitude of the moment in the ferromagnetic phase is also likely to grow even larger than the experimental moment.

In order to obtain the correct moment with the IC calculations a rather sizable crystal field is required and the parameter B_4 used to achieve this is negative (implying that Γ_8 is the ground state). The size of the crystal-field splitting is large compared to the ordering temperature and this may suggest that the crystal field should be introduced into the theory before the hybridization-mediated interaction is introduced as a perturbation. However, as in[27] CeSb, the single-ion effect of the hybridization presumably pushes the Γ_8 state down in energy toward the Γ_7 state (which is the ground state in a point-charge crystal-electric-field model), as the hybridization affects the Γ_8 state selectively and reduces its energy.[27] Therefore, the apparent large negative crystal-field splitting may just be a reflection of a strong Coqblin-Schrieffer (CS) hybridization rather than a large bare crystal-field effect. At least some of this single-ion effect should be included in the direct scattering included in Eq. (7), but this might not be an adequate treatment of the single-ion effect. The large crystal-field parameter required to match experimental values incorporates the remaining single-ion correction as well as the bare crystal-field effect.

If the bare crystal field is indeed larger than or comparable to the hybridization-mediated CS coupling, we need to consider the CS interaction between crystal-field basis states. These states reflect the cubic symmetry of the crystal, and it might be hoped that working in this basis would produce an antiferromagnetic phase with the correct polarization. This reflection of the cubic symmetry would not, however, be the same as the effect of the cubic part of the mixing potential.

ACKNOWLEDGMENTS

This work was supported through the U. S. Department of Energy under Contract No. DE-AS05-83ER45022. We are grateful to G. H. Lander for valuable discussion of the role of intermediate intraionic coupling and for informing us of the results of the neutron-scattering form-factor experiments on PuSb.

APPENDIX A

In this appendix we briefly outline the calculation of the matrix elements of the spin-orbit Hamiltonian of Eq. (2).

We begin by labeling the states of the configuration l^n as $|\Omega)$, those of the configuration l^{n-1} as $|\bar{\Omega})$, and the states of the l^1 single-electron configuration as $|\omega)$. Then we may write

$$|\Omega)=\sum_{\bar{\Omega},\omega}(\bar{\Omega};\omega\,|\,\Omega)\,|\,\bar{\Omega})\,|\,\omega)\,, \tag{A1}$$

and the matrix elements of a single-electron operator $F=\sum_i f_i$ may then be written as

$$\begin{aligned}(\Omega\,|\,F\,|\,\Omega')&=n(\Omega\,|\,f\,|\,\Omega')\\&=n\sum_{\bar{\Omega},\omega,\omega'}(\Omega\,|\,\bar{\Omega};\omega)(\omega\,|\,f\,|\,\omega')(\bar{\Omega};\omega'\,|\,\Omega')\,.\end{aligned} \tag{A2}$$

The problem then reduces to one of finding the coefficients $(\Omega\,|\,\bar{\Omega};\omega)$. These coefficients can be factorized as

$$\begin{aligned}(\bar{\Omega};\,\omega\,|\,\Omega)\equiv&(\bar{W}\,\bar{U}\,\bar{\tau}\,\bar{L}\,\bar{M}_L\bar{S}\,\bar{M}_S;lm_lm_s\,|\,WU\tau LM_LSM_S)\\=&(\bar{L}\,\bar{M}_L lm_l\,|\,\bar{L}lLM_L)(\bar{S}\,\bar{M}_S sm_s\,|\,\bar{S}sSM_S)\\&\times(\bar{W}\,\bar{U}\,\bar{\tau}\,\bar{L}+l\,|\,WU\tau L)\\&\times(l^{n-1}\bar{\nu}\,\bar{S}+l\,|\,\}l^n\nu S)\,,\end{aligned} \tag{A3}$$

where ν labels the "seniority" of the state. The part remaining after the two Clebsch-Gordan coefficients have been factored out is called a "coefficient of fractional parentage," usually abbreviated to cfp. For f electrons the first factor in the cfp can be further factorized as

$$\begin{aligned}(\bar{W}\,\bar{U}\,\bar{\tau}\,\bar{L}+l\,|\,WU\tau L)=&(\bar{U}\,\bar{\tau}\,\bar{L}+f\,|\,U\tau L)\\&\times(\bar{W}\,\bar{U}+f\,|\,WU)\,.\end{aligned} \tag{A4}$$

These two factors have been tabulated by Racah,[17] Judd,[14] and Wybourne[18] and the quantity $(f^{n-1}\bar{\nu}\,\bar{S}+f\,|\,\}f^n\nu S)$ can be easily calculated using expressions given by Judd.[14] Then the matrix elements of the spin-orbit Hamiltonian of Eq. (2) may be written as

$$\begin{aligned}(l^nWU\tau SLJM_J\,|\,\mathscr{H}_{\text{s.o.}}\,|\,l^nW'U'\tau'S'L'J'M'_J)=&\zeta\delta(J,J')\delta(M_J,M'_J)(-1)^{S'+L+J}[l(l+1)(2l+1)]^{1/2}\\&\times\begin{Bmatrix}S&S'&1\\L'&L&J\end{Bmatrix}(l^nWU\tau SL\,||\mathrm{W}^{(11)}||\,l^nW'U'\tau'S'L')\,,\end{aligned} \tag{A5}$$

where ζ is a radial integral usually treated as an experimentally determined parameter and the last quantity is the reduced matrix element of the tensor operator $W^{(11)}$. We have used the value of ζ quoted by Chan and Lam.[15] The reduced matrix elements may be written as

$$(l^n WU\tau SL||W^{(11)}||l^n W'U'\tau'S'L')=3n([S][S'][L][L'])^{1/2}(-1)^{1/2+l+S+L}$$

$$\times\sum_{\bar{\theta}}(\theta\{|\bar{\theta})(\theta'\{|\bar{\theta})(-1)^{\bar{S}+\bar{L}}\begin{Bmatrix} S & 1 & S' \\ \frac{1}{2} & \bar{S} & \frac{1}{2}\end{Bmatrix}\begin{Bmatrix} L & 1 & L' \\ l & \bar{L} & l\end{Bmatrix}, \tag{A6}$$

where $[a]=(2a+1)!$, $|\bar{\theta})\equiv|l^{n-1}\bar{W}\,\bar{U}\bar{\tau}\bar{S}\,\bar{L})$ is a parent term of $|\theta)\equiv|l^n WU\tau SL)$, and $(\theta\{|\bar{\theta})$ is the relevant cfp.

APPENDIX B

In order to determine the scattering coefficients $A_{mm'}^{MM'}$ which arise in our theory[11,12] [see Eq. (6)] we need to express the different degenerate ground-state wave functions as linear combinations of Slater determinants. Here we present an outline of the calculations involved in obtaining such linear combinations. The relevant linear combinations are easily obtained in the L-S coupling limit because the ^6H state with the highest values of $|M_L|$ and $|M_S|$ contains only one SD, which can be easily found by inspection. The states with other M_L and M_S can then be found by using the raising and lowering operators $L_\pm$ and $S_\pm$. In the IC case we need to find, in addition, the linear combinations of SD's corresponding to the ^4G states.

In order to determine the linear combination of Slater determinants corresponding to a state with given values of L and S, it is simplest to start by determining all the SD's which have the largest values of $|M_L|$ and $|M_S|$ compatible with the given L and S. Then one needs to obtain the matrix elements of L^2 and of S^2 between these SD's and diagonalize the resulting matrix of L^2+S^2, i.e., simultaneously diagonalize L^2 and S^2. It is then possible to pick out the eigenvectors corresponding to the required values of L and S. (Note that one can diagonalize L^2+S^2 and consequently diagonalize L^2 and S^2 simultaneously, rather than diagonalizing L^2 and S^2 sequentially, because one has selected a set of SD's that belong to L and S equal to or greater than the L and S of interest.) Linear combinations for other $|LSM_LM_S)$ states can then be found by using the spin and orbital angular momentum raising and lowering operators.

When there are many distinct states with the same L and S, we need to carry this procedure further in order to obtain a unique linear combination of SD's for each state. To do this we note that L^2 is the Casimir operator for the group R(3). The other quantum numbers that distinguish the states with common values of L and S label irreducible representations of the groups G(2) and R(7). Hence, we need to diagonalize the matrices for the Casimir operators of these groups along with L^2 and S^2. We can then pick out the eigenvectors corresponding to the required values of $WUSL$ and thus obtain a unique linear combination of SD's for each of the ^4G states.

The general one-electron spherical tensor operator of rank k is defined so that its reduced matrix element is given by

$$(nl||v^{(k)}||n'l')=(2k+1)^{1/2}\delta(n,n')\delta(l,l')\ . \tag{B1}$$

Then the effect of the qth component of the tensor operator on a one-electron state can be expressed as

$$v_q^{(k)}|lm_l)=\sum_{m_l'}(-1)^{l-m_l'}(2k+1)^{1/2}\times\begin{pmatrix} l & k & l \\ -m_l' & q & m_l\end{pmatrix}|lm_l')\ . \tag{B2}$$

For configurations l^n with more than one electron, we can, in analogy with angular momentum operators, define

$$V_q^{(k)}=\sum_{i=1}^{n}(v_q^{(k)})_i\ . \tag{B3}$$

For the case of f-electron configurations, the tensor operators $V^{(1)}$, $V^{(3)}$, and $V^{(5)}$ serve as generators for the group R(7), and $V^{(1)}$ and $V^{(5)}$ serve as generators for the group G(2).

If we denote the generators of any continuous group by X_μ, and the metric tensor in the weight space by $g_{\mu\nu}$, the Casimir operator for the group is defined as

$$\mathscr{C}=g^{\mu\nu}X_\mu X_\nu\ . \tag{B4}$$

The Casimir operators for R(7) and G(2) are then given by

$$\mathscr{C}[\mathrm{R}(7)]=\tfrac{1}{5}\sum_{k\ \mathrm{odd}}(V^{(k)})^2 \tag{B5a}$$

and

$$\mathscr{C}[\mathrm{G}(2)]=\tfrac{1}{4}[(V^{(1)})^2+(V^{(5)})^2]\ , \tag{B5b}$$

respectively. The squares of the tensor operators are defined in the usual way,

$$(V^{(k)})^2=\sum_i[(v^{(k)})_i]^2+2\sum_{\substack{i,j\\ i>j}}(v^{(k)})_i\cdot(v^{(k)})_j\ , \tag{B6a}$$

where

$$(v^{(k)})_i^2=(v^{(k)})_i\cdot(v^{(k)})_i \tag{B6b}$$

and

$$(v^{(k)})_i \cdot (v^{(k)})_j = \sum_q (-1)^q (v_q^{(k)})_i (v_{-q}^{(k)})_j \ . \qquad \text{(B6c)}$$

Combining this with Eq. (B2) one can calculate the matrix elements of the two relevant Casimir operators. In addition to tensor operators that change the magnetic quantum numbers of individual electrons by ± 1 (the familiar angular momentum raising and lowering operators, which are related to the operators $V_{\pm 1}^{(1)}$), one now has to contend with operators that may change the individual magnetic quantum numbers by as much as ± 5.

[1]J. Rossat-Mignod, P. Burlet, S. Quezel, and O. Vogt, Physica **102B**, 237 (1980).

[2]P. Burlet, S. Quezel, J. Rossat-Mignod, O. Vogt, J. C. Spirlet, and J. Rebizant, in Proceedings of the 13th Journées des Actinides, Elat, Israel, 1983 (unpublished).

[3]G. Busch and O. Vogt, Phys. Lett. **25A**, 449 (1967); Bernard R. Cooper, M. Landolt, and O. Vogt, in *Proceedings of the International Conference on Magnetism—Moscow,* edited by R. P. Ozerov and Yu. A. Izyumov (Nauka, Moscow, 1974), Vol. 5, pp. 354—360.

[4]J. C. Spirlet, J. Rebizant, and O. Vogt, in Proceedings of the 13th Journées des Actinides, Elat, Israel, 1983 (unpublished).

[5]J. Rossat-Mignod, P. Burlet, J. Villain, H. Bartholin, T. S. Wang, and D. Florence, Phys. Rev. B **16**, 440 (1977); P. Fischer, B. Lebech, G. Meier, B. D. Rainford, and O. Vogt, J. Phys. C **11**, 345 (1978).

[6]R. Siemann and Bernard R. Cooper, Phys. Rev. Lett. **44**, 1015 (1980).

[7]Bernard R. Cooper, J. Magn. Magn. Mater. **29**, 230 (1982).

[8]David Yang and Bernard R. Cooper, J. Appl. Phys. **53**, 1988 (1982).

[9]Bernard R. Cooper, P. Thayamballi, and D. Yang, J. Appl. Phys. **55**, 1866 (1984); P. Thayamballi, D. Yang, and B. R. Cooper, Phys. Rev. B **29**, 4049 (1984).

[10]B. Coqblin and J. R. Schrieffer, Phys. Rev. **185**, 847 (1969).

[11]P. Thayamballi and Bernard R. Cooper, J. Appl. Phys. **53**, 7902 (1982).

[12]P. Thayamballi and Bernard R. Cooper, J. Appl. Phys. **55**, 1829 (1984).

[13]Bernard R. Cooper, P. Thayamballi, J. C. Spirlet, W. Müller, and O. Vogt, Phys. Rev. Lett. **51**, 2418 (1983).

[14]Brian Judd, *Operator Techniques for Atomic Spectroscopy* (McGraw-Hill, New York, 1963).

[15]S. K. Chan and D. J. Lam, in *The Actinides,* edited by A. Freeman and J. Darby (Academic, New York, 1974) Vol. 1.

[16]E. U. Condon and G. H. Shortley, *The Theory of Atomic Spectra* (MacMillan, New York, 1935).

[17]Giulio Racah, Phys. Rev. **61**, 186 (1942); **62**, 438 (1942); **63**, 367 (1943); **76**, 1352 (1949).

[18]B. G. Wybourne, J. Chem. Phys. **35**, 334 (1961); **35**, 340 (1961); **36**, 2295 (1962); **36**, 2301 (1962).

[19]David Yang and Bernard R. Cooper, J. Appl. Phys. **52**, 2234 (1981).

[20]P. W. Anderson, Phys. Rev. **124**, 41 (1961).

[21]J. R. Schrieffer, J. Appl. Phys. **38**, 1143 (1967).

[22]J. R. Schrieffer and P. A. Wolff, Phys. Rev. **149**, 491 (1966).

[23]M. A. Ruderman and C. Kittel, Phys. Rev. **96**, 99 (1954).

[24]M. Tinkham, *Group Theory and Quantum Mechanics* (McGraw-Hill, New York, 1964).

[25]This is the value from recent neutron-scattering form-factor measurements performed by G. H. Lander, A. Delapalme, P. J. Brown, J. C. Spirlet, and O. Vogt, in Proceedings of the Journées des Actinides, Davos, Switzerland, 1984 (unpublished) (available from Dr. J. Schoenes, Laboratorie für Festkörperphysik, Eidgenössche Technishe Hochschule, CH-8093 Zürich, Switzerland). As is typically the case for light actinide compounds, this differs from the total moment measured in magnetization experiments as reported in Refs. 4 and 13, presumably because of antiparallel polarization of the band electron moment.

[26]K. R. Lea, M. J. M. Leask, and W. P. Wolf, J. Phys. Chem. Solids **23**, 1381 (1962).

[27]K. Takegahara, H. Takahashi, A. Yanase, and T. Kasuya, Solid State Commun. **39**, 857 (1981).